Terra Nova

doi: 10.1111/ter.12178

Inferring autogenically induced depositional discontinuities from observations on experimental deltaic shoreline trajectories

Daniel Mikeš,[1] Johan H. ten Veen,[2] George Postma[3] and Ronald Steel[4]

[1]*Department of Geosciences, Nelson Mandela Metropolitan University, PO Box 77000, Port Elizabeth 6031, South Africa;* [2]*TNO – Geological Survey of the Netherlands, PO Box 80015, Utrecht 3508 TA, The Netherlands;* [3]*Faculty of Geosciences, Utrecht University, PO Box 80021, Utrecht 3508 TA, The Netherlands;* [4]*Jackson School of Geosciences, University of Texas at Austin, Austin TX 78712, USA*

ABSTRACT

Palaeo shoreline is a commonly used proxy for palaeo sea level, but only if deposition is continuous and constant will shoreline trajectory *T*(*l*) completely capture sea-level time-series *E*(*t*). Artificial deltas were generated in the Eurotank flume facility under stepwise tectonic subsidence, periodic sea-level fluctuation and two periodic water-discharge scenarios, one in-phase and the other out-of-phase with sea level. Independent input variables tectonic subsidence *Y*, sea level *E* and water discharge *Q* (controlling sediment supply *S*) were varied and dependent output variable shoreline trajectory *T* was monitored. These experiments confirm that deposition is discontinuous even for continuous sediment supply, and this hinders the inference of sea-level curve from shoreline trajectory. These results justify the here-developed methodology for converting shoreline trajectory from the space domain to the time domain, thereby improving the accuracy of the inferred sea-level curve.

Terra Nova, 27, 442–448, 2015

Introduction

A fundamental goal in process sedimentology at the deposystem scale is to reconstruct deposystem kinetics, i.e. infer deposystem evolution through time from the ensuing stratal anatomy and identify the key drivers involved. This procedure is hindered by the complexity of the functional relations between independent and dependent variables. Many of these relations have been addressed by a great number of researchers: modelling of deposystems (Paola *et al.*, 2009); experimental scaling (Schumm *et al.*, 1987; Paola *et al.*, 1992, 2009; Peakall *et al.*, 1996; Paola, 2000; van Heijst and Postma, 2001; Castelltort and van den Driessche, 2003; Postma *et al.*, 2008; Kleinhans *et al.*, 2014); autogenic mechanisms (Tipper, 2000; Muto and Swenson, 2006; Kim and Paola, 2007; Muto *et al.*, 2007; Nicholas and Quine, 2007; van Dijk *et al.*, 2009; Karamitopoulos *et al.*, 2014; Leva López *et al.*, 2014); allogenic controls on shoreline (Pitman, 1978; Muto and Steel, 1997; Kim *et al.*, 2006b); autogenic controls on shoreline (Muto and Steel, 2001, 2002; Kim *et al.*, 2006a; Kleinhans *et al.*, 2014); discharge control on supply (Leeder *et al.*, 1998; van der Zwan, 2002; van den Berg van Saparoea and Postma, 2008; Postma and van den Berg van Saparoea, 2008); discharge and supply control on stratigraphy (Postma and van den Berg van Saparoea, 2008; Carvajal *et al.*, 2009); supply control on accumulation (Tipper, 1983, 1998, 2002, 2014; Kemp, 2012; Kemp and Sexton, 2014); accumulation (Sadler, 1981, 1994, 1999; Sadler and Strauss, 1990; Kemp and Sexton, 2014); multivariate control (Heller *et al.*, 2001; Kim *et al.*, 2006b; Burgess *et al.*, 2008; Postma and van den Berg van Saparoea, 2008; Burgess and Prince, 2014); prediction vs. inference (Paola, 2013); supply vs. sea level (Muto and Steel, 1997; Burgess and Hovius, 1998; Perlmutter *et al.*, 1998; Carvajal *et al.*, 2009; Bijkerk *et al.*, 2014); and sea-level curve vs. shoreline trajectory (Pitman, 1978; Martin *et al.*, 2009).

Despite the importance of all these studies, the occurrence of autogenically induced depositional discontinuities and their effect on the inference of input from output is still under-explored. Autogenic mechanisms cause discontinuities in local sediment supply (flux) (Kim *et al.*, 2006b), which in turn cause discontinuities in deposition (accumulation) and preservation. These discontinuities affect shoreline trajectory, because they interrupt the recording of sea level and therefore render the reconstructed shoreline trajectory incomplete. To what extent these discontinuities hinder the inference of sea level from shoreline trajectory is the main question addressed in this study. We choose to use analogue experiments, because they might reveal unexpected behaviour. Miniature deposystem kinetics are sufficiently similar to natural systems to answer this particular question (Postma *et al.*, 2008).

In this pilot study, we investigate input (independent variables) and output (dependent variables). By means of two miniature delta scenarios in a flume tank under controlled conditions (Fig. 1) we studied the tie between input and output. These scenarios were chosen quite arbitrarily, since the study aimed to explore general relations between input and output rather than simulating specific natural deltas. The key question to be addressed here is: 'Do autogenic mechanisms significantly affect shoreline trajectory?'. To explore this question, we tested in particular whether shoreline length-series $T(l)$ match shoreline time-series $T(t)$ [and sea-level time-series $E(t)$]. If they do, the functional relation between sea level and shoreline is simple, and one can easily infer the sea-level curve

Correspondence: Professor Daniel Mikeš, Department of Geosciences, Nelson Mandela Metropolitan University, PO Box 77000, Port Elizabeth 6031, South Africa. Tel.: +27 (0)41 504 2243; fax: +27 (0)41 504 23 40; e-mails: dmikes@nmmu.ac.za; danmikes @gmail.com.

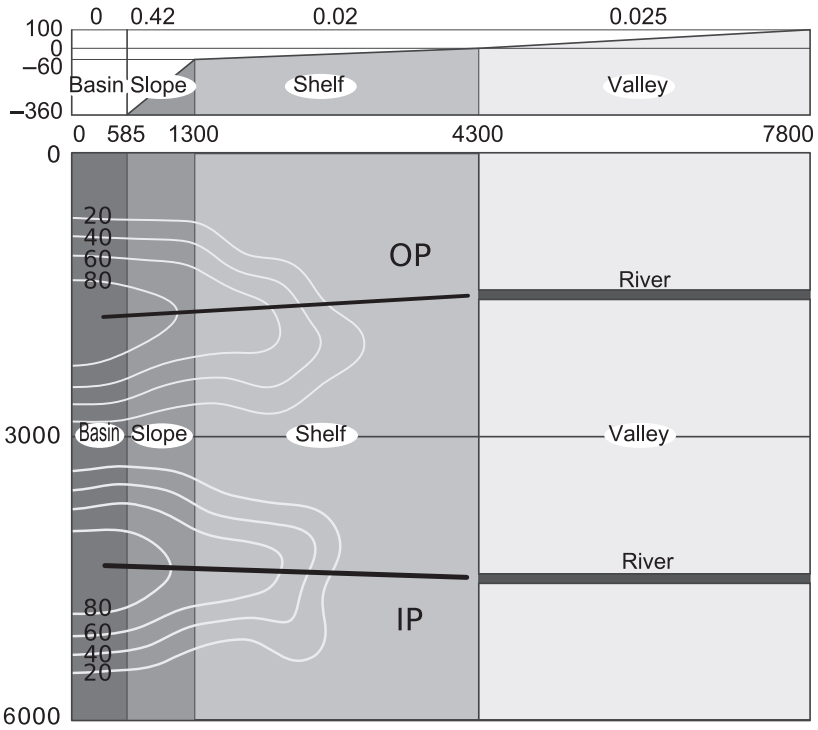

Fig. 1 Experimental set-up in profile and plan view. OP: sea-level and sediment-supply changes are out-of-phase; IP: sea level and sediment supply are in-phase; units above profile are *gradients*; all other units are *mm*; white contour lines denote cumulative subsidence at the end of the experiment; black radial lines denote the locations of cross-sections (Fig. 2).

from shoreline trajectory; if they don't, the functional relation between them is complex, and one cannot fully infer the sea-level curve from shoreline trajectory.

Input

Tectonic subsidence Y simulates thermal subsidence of a passive margin, which, due to the design of the set-up, was applied in a stepwise manner. Water-level variation E in the tank simulates variation in global sea level following part of a typical Milankovitch-type insolation curve with variable amplitude as a proxy for glacioeustasy. Although the occurrence of glacials–interglacials depends on periodic changes in insolation, the applied one-to-one relation is probably over-simplified (e.g. Zachos *et al*., 2001). The joint effect of subsidence and water-level variations yields an asymmetric base-level curve B, with faster rise than fall (Bijkerk *et al*., 2014). Sediment supply S to the delta simulates regional sediment-supply variations driven by climatic variations (Leeder *et al*., 1998). However, in this flume tank set-up, supply changes cannot be controlled directly, but instead need to be regulated by varying water discharge Q, which in turn causes regional sediment supply to vary. Regional sediment supply is used for the sediment flux at the delta apex; local sediment supply is used for the sediment flux at a location on the delta.

Two simultaneous model scenarios were run, each with a different periodic water-discharge fluctuation: (1) supply increasing with rising sea level (in-phase – IP); (2) and supply decreasing with rising sea level (out-of-phase – OP). For both scenarios, the same semi-constant tectonic subsidence and periodic sea-level fluctuation were applied. Individual autogenic processes in the delta are not discerned, but are represented by one virtual parameter L, which is not measured or defined by a particular process, but encompasses any mechanism other than the controlled drivers. In this case, however, animations from photographs indicate that lobe switching via channel avulsion was the dominant autogenic mechanism. Autogenic drivers cause local sediment supply S fluctuations, which in turn cause depositional fluctuations.

Order is used generically and relatively, i.e. higher order indicates higher frequency; first order in this case corresponds to the sea-level cycle. Sea level is used for the water level from a fixed datum, and base level (relative sea level) for the water level from basement. Shoreline position is indicated by its horizontal distance from the delta apex. The term 'length-series' is used to distinguish shoreline position against ordinal lamina number [length-series in length units (l)] from shoreline position against time [time-series in time units (t)]. Shoreline position T (brink-, rollover-, inflexion point of the clinoform) is the monitored output parameter. The brink point is taken to coincide with the shoreline, although in reality it corresponds to a distributary channel base ~ 2–10 mm below water level.

Method

In the Eurotank, two deltas prograded onto a scaled continental shelf (Fig. 1). Tectonic subsidence was applied incrementally by lowering the hexagonal blocks of the tank floor; hence, the net subsidence rate was pseudo-constant $Y \propto t$ and equal for the in-phase and out-of-phase scenarios $Y_{IP} = Y_{OP}$. Water level was changed by lowering the tank's overflow. Water discharge was changed by valves. Tectonic subsidence and sediment supply were monitored at ~3.5 h intervals; water level and water discharge were monitored at 0.2 h intervals. In the IP scenario, water discharge mimics sea level proportionally $Q_{IP} \propto E$, whereas in the OP scenario water discharge mirrors sea level proportionally $Q_{OP} \propto -E$. Sediment was introduced at the head of the river at a constant rate through a sediment feeder. For further details on the set-up see Bijkerk *et al*. (2014).

Water-discharge fluctuations cause the river system to modulate the constant sediment supply to the river.

Increasing water discharge decreases the river gradient, causing erosion in the river, therewith increasing sediment supply S to the delta; decreasing water discharge increases the river gradient, causing deposition in the river, and decreasing the regional sediment supply S to the delta. As a result, regional sediment supply to the delta is approximately proportional to water discharge $S \propto Q$ (van den Berg van Saparoea and Postma, 2008; Postma and van den Berg van Saparoea, 2008). This causes the regional sediment supply to the delta to fluctuate in-phase $S_{IP} \propto E$ and out-of-phase $S_{OP} \propto -E$ with sea level respectively (Leeder *et al.*, 1998; Perlmutter and Plotnick, 2003). Actual sediment supply was calculated from elevation profiles through the river channel. Coloured tracer sands were spread at times of sea-level highs and lows $t \in (0; 2.5; 17.5; 25; 32.5; 42.5)$ hours to provide time markers and to denote transgressive and regressive intervals on the lacquer peels (sea-level trends in Fig. 2).

Cross-sections through the delta were produced by making radial lacquer peels through the apex and along the centre of the delta on which stratal terminations of laminae (downlap, offlap, onlap, toplap) and shoreline positions (brink-/rollover-/inflexion points) of all laminae were marked in chronologic order (black dots on shoreline trends in Fig. 2). Shoreline trajectory is defined as the angle of the segment between two brink points (Fig. 3) with 0 vertically up, yielding positive values for regression and negative values for transgression (Fig. 3), slightly modifying the original concept (cf Helland-Hansen and Martinsen, 1996). Shoreline position is defined as the distance of the shoreline from the delta apex. Shoreline position is tuned to time markers (colour tracers) and plotted against time t to generate the shoreline time-series $T(t)$. Shoreline position T is plotted against ordinal lamina number n to generate the shoreline length-series $T(l)$. For shoreline trajectory $\dot{T}$ six stratotypes are identified, four subaqueous delta-front stratotypes, including shoreline (Figs 2 and 3), and two subaqueous/subaerial delta-top stratotypes landward of the shoreline (Fig. 2). The ensuing sequence analysis along the axial lacquer peels is shown in Fig. 2.

All series are plotted in Fig. 4, i.e. time-series of the regional input variables, namely: tectonic subsidence $Y(t)$, sea level $E(t)$ and measured regional sediment supply $S(t)$ (Fig. 4A); time- and length-series of the output variable shoreline position $T(t)$ and $T(l)$ (Fig. 4B); and length-series of the shoreline trajectory $\dot{T}(l)$ (Fig. 4C). Most values for the shoreline trajectory fall between −90 and 90, but extreme outliers between −180 and 180 do occur. Time-series are 'tuned' to absolute time using the tracer sands, i.e. at $t \in (0; 2.5; 17.5; 25; 32.5; 42.5)$ hours; between time markers laminae are distributed evenly over the interval, ignoring any hiatus. Length-series are not 'tuned' to time: all laminae are distributed evenly between the start and end of the experiment as if they were deposited at regular time intervals. Time- and length-series are thus similar to a Wheeler diagram representation of shoreline positions obtained from a cross-section or seismic line.

Results

Sea-level trends (Fig. 2) exhibit few differences between IP and OP, save for slightly more transgressive relative to regressive deposits in IP than in OP. Shoreline trends exhibit many similarities and differences between IP and OP (Fig. 2). The similarities are (1) maximum transgressions MT coincide with sea-level highs and maximum regressions with sea-level lows; and (2) erosional unconformities EU occur before sea-level lows. The differences are: (1) IP has a more uniform stratal appearance than OP, i.e. IP has fewer stratal units than OP; (2) IP has smaller shoreline shifts than OP; (3) IP has more transgressive deposits than OP; and (4) IP has less regressive deposits than OP.

Shoreline trajectories also exhibit many similarities and differences between IP and OP (Fig. 4). The similarities are: (1) both scenarios have large abrupt transgressions, notably in intervals 15−25 h and 30−40 h (Fig. 4B,C), due to tectonic-subsidence steps (Fig. 4A); and (2) both scenarios have smaller abrupt transgressions, over the larger ones, due to autogenics; for example subsidence during abandonment of a mouth bar might create a transgression after its return. The differences are: (1) tectonically induced transgressions are less extensive in IP than in OP (Fig. 4B); (2) autogenically induced transgressions are more numerous in IP than in OP (Fig. 4B); and (3) shoreline trajectory maxima occur at different 'times' in IP and OP (Fig. 4C).

Local sediment-supply fluctuations cause a significant offset of peaks in shoreline position (Fig. 4B) between time-series and length-series, notably between 10 and 15 h in both scenarios, between 20 and 25 h for IP and between 35 and 40 h for OP. Moreover, shoreline trajectories show additional higher-order cycles during transgressions (Fig. 4B). Some of these seem to be caused by tectonic-subsidence jumps, e.g. at times 2, 17.5, 23, 24, 25, 34, 36, 37 and 40 h for IP and at 7.5, 19, 23, 25, 35 and 38 h for OP. As there are more shoreline jumps than tectonic jumps, some were caused by depositional discontinuities, i.e. deposition returning to a location after a hiatus during a sea-level rise, causing an abrupt transgression.

Visual inspection of photographs taken every 0.2 h reveals that the depo-ratio, i.e. the ratio of depositional intervals to hiatus intervals, is ~ 0.2, i.e. 20% of the time there is deposition, meaning that the hiatus-ratio is ~ 0.8, i.e. 80% of the time there is no deposition (Berry, 2012). Intervals of non-deposition vary in spacing and duration.

The results show that first-order shoreline cycles mimic sea-level cycles, but allogenics (tectonic subsidence and regional sediment supply) and autogenics (lobe switching) modulate shoreline shifts: (1) in both scenarios tectonic-subsidence jumps cause large abrupt transgressions; (2) in both scenarios autogenic mechanisms (predominantly lobe switching) cause small abrupt transgressions over the tectonically induced ones; (3) in both scenarios autogenic lobe switching causes local depositional discontinuities, which in turn cause offsets in the transgressions between the shoreline length-series and the sea-level time-series (10–15 h for IP and OP, 20–25 h for IP and 35–40 h

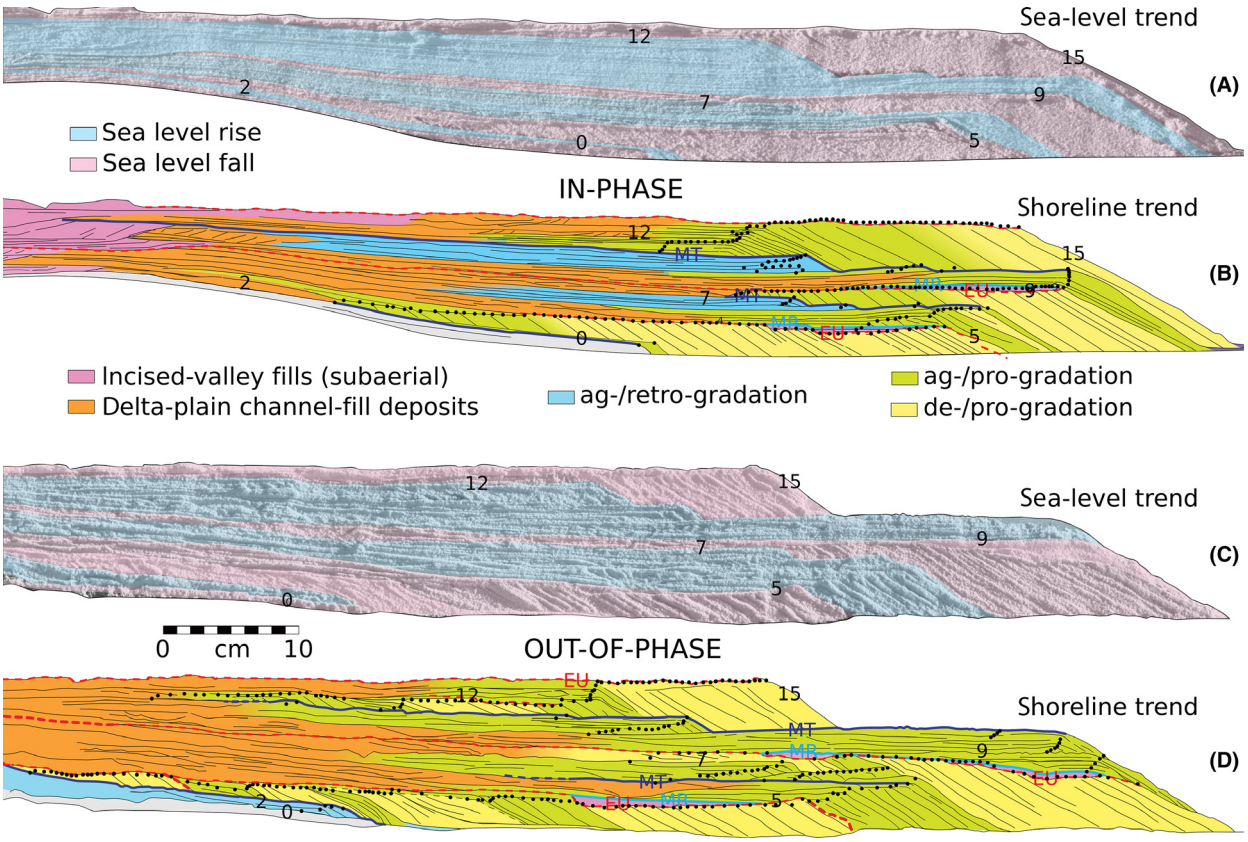

Fig. 2 Central lacquer peels generated in the experiments, and their interpretation. (A) In-phase sea level and water discharge (cyan = rise, magenta = fall); (B) in-phase stratotype and shoreline trajectory; (C) out-of-phase sea level and water discharge; (D) out-of-phase stratotype and shoreline trajectory. Cross-sections from lacquer peels (Fig. 1); subaqueous stratotypes are denoted according to shoreline trajectory nomenclature (Fig. 3); subaerial stratotypes are denoted according to different styles of fluvial deposition (incised valley-fills and delta-plain channel fills); heavy dots denote shoreline position for each lamina; numbers denote time steps $\tilde{t} \in (0; 2; 5; 7; 9; 12; 15)$ (Fig. 4), which correspond to marker sands in the lacquer peels at $t \in (0; 2.5; 17.5; 25; 32.5; 42.5)$ hours; MT, maximum transgression; MR, maximum regression; EU, erosional unconformity.

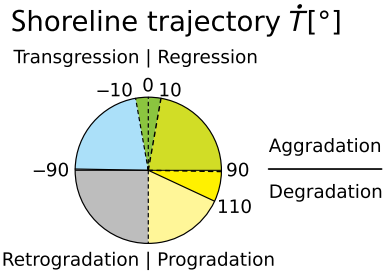

Fig. 3 Stratotype classification of subaqueous stratotypes based on shoreline trajectory. (A) −90 to −10 = aggradation + retrogradation; (B) −10 to 10 = aggradation; (C) 10 to 90 = aggradation + progradation; (D) 90 to 110 = degradation + progradation. Adapted from Helland-Hansen and Martinsen (1996).

for OP); (4) IP variation in sediment supply attenuates shoreline shift, whereas OP variation amplifies it (Fig. 4B); this causes shifts in shoreline to be smaller for IP than for OP.

Discussion

The deltas that formed in the tank are similar to natural coarse-grained fan deltas (van Dijk *et al.*, 2009): they were fed from a point source (the river channel) while sediment transport produced a fan-shaped delta plain by stream crevassing (much like that occurring on alluvial fans). The delta front is characterized by steep foresets formed by sediment avalanching down the delta front onto the shelf. As in present-day deltas, the shoreline coincides with the brinkpoint between the gentle gradient of the delta plain and the steep gradient of the delta front. Shoreline trajectories obtained from our laboratory experiments thus are similar to shoreline trajectories reconstructed from seismic lines (Helland-Hansen and Martinsen, 1996). Shifting of distributaries by avulsion produces local differences in delta progradation rates and local discontinuities in the stratigraphic record.

The results confirm again that even the simplest deltas are complex. Although shoreline cycles follow first-order sea-level cycles, they also exhibit additional higher-order cycles caused by allogenic depositional discontinuity responses. If one were to infer the sea-level time-series from the shoreline trajectory length-series, one might erroneously postulate higher-order sea-level cycles. Moreover, for natural systems there will be no perfectly radial cross-sections, and it is likely that facies would be used to infer shoreline cycles,

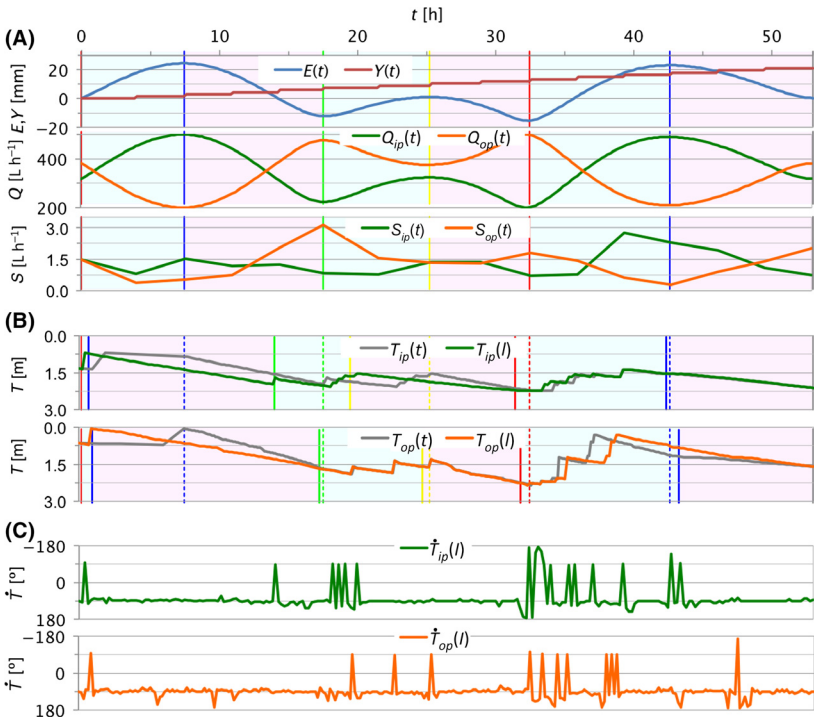

Fig. 4 Input and output series: ip = in-phase; op = out-of-phase. (A) True time-series of global input signals eustasy $E(t)$, tectonic subsidence $Y(t)$, water discharge $Q(t)$ and sediment supply $S(t)$; cyan areas denote sea-level rises, magenta areas denote sea-level falls. (B) Time-series $T(t)$ and length-series $T(l)$ of shoreline position [distance from delta apex (0, 0)] for central cross-sections, time-series tuned to time at $t \in (0; 2.5; 17.5; 25; 32.5; 42.5)$ hours, length-series not tuned to time; dotted vertical lines denote true time of markers, solid vertical lines denote apparent time of markers from length-series. (C) Length-series $\dot{T}(l)$ of shoreline trajectory [angle between two subsequent shoreline points in lacquer peel (Fig. 3)].

increasing the reconstruction difficulty.

The results strongly suggest that autogenic local-supply variations can affect shoreline trajectory in two ways: (1) discontinuities in the shoreline trajectory; and (2) additional transgressions/regressions. In the case of climatically steered sea-level and sediment-supply fluctuations, the responses are similar overall, but different in details. Therefore, ignoring depositional discontinuities might lead to an incorrect inference of sea-level cycles. It is too early to provide a quantitative analysis, but one can speculate on the errors, challenges and opportunities of inferring the sea-level curve from the shoreline trajectory for these deltas.

If one were to infer a sea-level curve from these lacquer peels, one might infer an incorrect sea-level cycle period of up to a quarter period. Deposition in lacquer peels away from the delta apex would be even less complete, and the error would only increase. And this is still for these experiments, with a continuous regional sediment supply. For a discontinuous regional supply, as in natural systems, the error would further increase. By how much remains a question for now, but this should be addressed in the near future. Once the quantitative relation between sea-level curve and shoreline trajectory is known, one can explore the possibilities of the inverse relation – that is to say converting the shoreline trajectory from the space domain to the time domain.

Concluding remarks

Both allogenic and autogenic drivers affect shoreline behaviour in a complex way. These experiments suggest that, at least at tank scale, regional (allogenic) and local (autogenic) sediment-supply fluctuations also affect shoreline shifts: $S \rightarrow T$. Those in-phase with sea level attenuate the shoreline shifts, whereas those out-of-phase with sea level amplify the shoreline shifts. Shoreline length-series do not match shoreline time-series: $T(l) \not\propto T(t)$; and therefore shoreline time-series do not match sea-level time-series: $T(t) \not\propto E(t)$; events (transgressive peaks) show significant offsets. Tuned time-series correct large offsets, but not small ones. These findings suggest that, without dense time-control, one cannot infer sea-level cycles from shoreline cycles $E \not\leftrightarrow T$.

The results show that higher-order shoreline cycles might be incorrectly interpreted as higher-order sea-level cycles, but are in reality autogenically controlled supply cycles. These findings also suggest that if the aim is to infer sea-level cycles from 2D sections it is necessary to choose shoreline measurement intervals that do not alias anticipated sea-level cycles or at the very least to understand the period of sea-level cycles that can be inferred from a given set of measurements. These results, coming on the heels of the autostratigraphy appeal (Muto *et al.*, 2007), suggest possible new avenues for analytic stratigraphic study.

Acknowledgements

We express gratitude to: M. van Dijk, T. van Gon Netcher, S. Hahn, H. van der Meer and F. Trappenburg for experiments; J. Bijkerk, M. Perillo and J. Tipper for pre-review; E. Thomas, P. Burgess and two anonymous reviewers for review from *Geology*; M. Coleman, W. Helland-Hansen, C. Paola, an anonymous reviewer and the anonymous Associate Editor for review from *Terra Nova*.

References

van den Berg van Saparoea, A.-P. and Postma, G., 2008. Control of climate change on the yield of river systems. In: *Recent Advances in Models of Siliciclastic Shallow-Marine Stratigraphy* (G. Hampson, R. Steel, P. Burgess and R. Dalrymple, eds). *Soc. Sediment. Geol. Spec. Publ.*, **90**, 15–33.

Berry, R., 2012. Signal analysis on hiatus pattern of artificial delta. BSc-hon thesis, Stellenbosch University.

Bijkerk, J., ten Veen, J., Postma, G., Mikeš, D., van Strien, W. and de Vries,

J., 2014. The role of climate variation in delta architecture: lessons from analogue modelling. *Basin Res.*, **26**(3), 351–368.
Burgess, P. and Hovius, N., 1998. Rates of delta progradation during highstands: consequences for timing of deposition in deep-marine systems. *J. Geol. Soc.*, **155**, 217–222.
Burgess, P. and Prince, G., 2015. Non-unique stratal geometries: implications for sequence stratigraphic interpretations. *Basin Res.*, **27**(3), 351–365.
Burgess, P., Steel, R. and Granjeon, D., 2008. Stratigraphic forward modeling of basin-margin clinoform systems: implications for controls on topset and shelf width and timing of formation of shelf-edge deltas. *SEPM Spec. Publ.*, **90**, 35–45.
Carvajal, C., Steel, R. and Petter, A., 2009. Sediment supply: the main driver of shelf-margin growth. *Earth-Sci. Rev.*, **96**, 221–248.
Castelltort, S. and van den Driessche, J., 2003. How plausible are high-frequency sediment-supply driven cycles in the stratigraphic record? *Sed. Geol.*, **157**(1), 3–13.
van Dijk, M., Postma, G. and Kleinhans, M., 2009. Autocyclic behaviour of fan deltas; an analogue experimental study. *Sedimentology*, **56**, 1569–1589.
van Heijst, M. and Postma, G., 2001. Fluvial response to sea-level changes: a quantitative analogue, experimental approach. *Basin Res.*, **13**, 269–292.
Helland-Hansen, W. and Martinsen, O., 1996. Shoreline trajectories and sequences: description of variable depositional dip scenarios. *J. Sediment. Res.*, **66**, 670–688.
Heller, P., Paola, C., Hwang, I., John, B. and Steel, R., 2001. Geomorphology and sequence stratigraphy due to slow and rapid base-level changes in an experimental subsiding basin (xes 96-1). *Bull. Am. Assoc. Petrol. Geol.*, **85**, 817–838.
Karamitopoulos, P., Weltje, G. and Dalman, R., 2014. Allogenic controls on autogenic variability in fluvio-deltaic systems: inferences from analysis of synthetic stratigraphy. *Basin Res.*, **26**(6), 767–779.
Kemp, D., 2012. Stochastic and deterministic controls on stratigraphic completeness and fidelity. *Int. J. Earth Sci. (Geologische Rundschau)*, **101**, 2225–2238.
Kemp, D. and Sexton, P., 2014. Time-scale uncertainty of abrupt events in the geologic record arising from unsteady sedimentation. *Geology*, **42** (10), 891–894.
Kim, W. and Paola, C., 2007. Long-period cyclic sedimentation with constant tectonic forcing in an experimental relay ramp. *Geology*, **35** (34), 331–334.
Kim, W., Paola, C., Swenson, J. and Voller, V., 2006a. Shoreline response to autogenic processes of sediment storage and release in the fluvial system. *J. Geophys. Res.*, **111**, F4.
Kim, W., Paola, C., Voller, V. and Swenson, J., 2006b. Experimental measurement of the relative importance of controls on shoreline migration. *J. Sediment. Res.*, **76**(2), 270–283.
Kleinhans, M., van Dijk, W., van de Lageweg, W., Hoyal, D., Markies, H., van Maarse-veen, M., Roosendaal, C., van Weesep, W., van Breemen, D., Hoendervoogt, R. and Cheshier, N., 2014. Quantifiable effectiveness of experimental scaling of river- and delta morphodynamics and stratigraphy. *Earth-Sci. Rev.*, **133**, 43–61.
Leeder, M., Harris, T. and Kirkby, M., 1998. Sediment supply and climate change: implications for basin stratigraphy. *Basin Res.*, **10**, 7–18.
Leva López, J., Kim, W. and Steel, R., 2014. Autoacceleration of clinoform progradation in foreland basins: theory and experiments. *Basin Res.*, **26**, 489–504.
Martin, J., Paola, C., Abreu, V., Neal, J. and Sheets, B., 2009. Sequence stratigraphy of experimental strata under known conditions of differential subsidence and variable base level. *Am. Assoc. Pet. Geol. Bull.*, **93**(4), 503–533.
Muto, T. and Steel, R., 1997. Principles of regression and transgression: the nature of the interplay between accommodation and sediment supply. *J. Sediment. Res.*, **67**(6), 994–1000.
Muto, T. and Steel, R., 2001. Shoreline autoretreat substantiated in flume experiments. *J. Sediment. Res.*, **71**(2), 246–254.
Muto, T. and Steel, R., 2002. Role of autoretreat and a/s changes in the understanding of deltaic shoreline trajectory: a semi-quantitative approach. *Basin Res.*, **14**, 303–318.
Muto, T. and Swenson, J., 2006. Autogenic attainment of large-scale alluvial grade with steady sea-level fall: an analog flume-tank experiment. *Geology*, **34**, 161–164.
Muto, T., Steel, R. and Swenson, J., 2007. Autostratigraphy: a framework norm for genetic stratigraphy. *J. Sediment. Res.*, **77**, 2–12.
Nicholas, A. and Quine, T., 2007. Modeling alluvial landform change in the absence of external environmental forcing. *Geology*, **35**(6), 527–530.
Paola, C., 2000. Quantitative models of sedimentary basin filling. *Sedimentology*, **47**(1), 121–178.
Paola, C., 2013. Is it possible to predict the past? *Lithosphere*, **5**(4), 450–451.
Paola, C., Heller, P. and Angevine, C., 1992. The large-scale dynamics of grain-size variation in alluvial basins, 1: theory. *Basin Res.*, **4**, 73–90.
Paola, C., Straub, K., Mohrig, D. and Reinhardt, L., 2009. The "unreasonable effectiveness" of stratigraphic and geomorphic experiments. *Earth-Sci. Rev.*, **97**, 1–43.
Peakall, J., Ashworth, P. and Best, J., 1996. Physical modelling in fluvial geomorphology: principles, applications and unresolved numbers. In: *The Scientific Nature of Geomorphology, Proceedings of the 27th Binghamton Symposium in Geomorphology* (B. Roads and C. Thorn, eds), pp. 221–254. Wiley & Sons.
Perlmutter, M. and Plotnick, R., 2003. Hemispheric assymetry of the marine stratigraphic record: conceptual proof of a unipolar icecap. In: *Climate Controls on Stratigraphy* (C. Cecil and N. Edgar, eds). *Soc. Sediment. Geol. Spec. Publ.*, **77**, 51–66.
Perlmutter, M., Radovich, R., Matthews, M. and Kendall, C., 1998. The impact of high-frequency sedimentation cycles on stratigraphic interpretation. In: *Sequence Stratigraphy* (K. Sandvik, F. Gradstein and N. Milton, eds). *Norw. Petrol. Soc. Spec. Publ.*, **8**, 141–170.
Pitman, W.I., 1978. Relationships between eustacy and stratigraphic sequences of passive margins. *Geol. Soc. Am. Bull.*, **89**, 1389–1403.
Postma, G. and van den Berg van Saparoea, A.-P., 2008. Impact of discharge, sediment flux and sea-level change on stratigraphic architecture of river valley - delta - shelf systems. *Int. Assoc. Sedimentol. Spec. Publ.*, **40**, 191–206.
Postma, G., Kleinhans, M., Meijer, X. and Eggenhuisen, J., 2008. Sediment transport in analogue flume models compared with real world sedimentary systems: a new look at scaling sedimentary systems evolution in a flume. *Sedimentology*, **55**, 1541–1557.
Sadler, P., 1981. Sediment accumulation rates and the completeness of stratigraphic sections. *J. Geol.*, **89**, 569–584.
Sadler, P., 1994. The expected duration of upward-shallowing peritidal carbonate cycles and their terminal hiatuses. *Geol. Soc. Am. Bull.*, **106**, 791–802.
Sadler, P., 1999. The influence of hiatuses on sediment accumulation rates. *GeoRes Forum*, **5**, 15–40.
Sadler, P. and Strauss, D., 1990. Estimation of completeness of

stratigraphical sections using empirical data and theoretical models. *J. Geol. Soc. London*, **147**, 471–485.

Schumm, S., Mosley, P. and Weaver, P., 1987. *Experimental Fluvial Geomorphology*. Wiley & Sons, 413 pp.

Tipper, J., 1983. Rates of sedimentation, and stratigraphical completeness. *Nature*, **302**(5910), 696–698.

Tipper, J., 1998. The influence of field sampling area on estimates of stratigraphic completeness. *J. Geol.*, **106**, 727–739.

Tipper, J., 2000. Patterns of stratigraphic cyclicity. *J. Sediment. Res.*, **70**(6), 1262–1279.

Tipper, J., 2002. A fractionation model for sediment delivery. In: *Sediment Flux to Basins: Causes, Controls and Consequences* (S. Jones and L. Frostick, eds). *Geol. Soc. London Spec. Publ.*, **191**, 161–170.

Tipper, J., 2014. The importance of doing nothing: stasis in sedimentation systems and its stratigraphic effects. In: *Strata and Time: Probing the Gaps in Our Understanding* (D. Smith, R. Bailey, P. Burgess and A. Fraser, eds). *Geol. Soc. London Spec. Publ.*, **404**, 105–122.

Zachos, J., Pagani, M., Sloan, L., Thomas, E. and Billups, K., 2001. Trends, rhythms, and aberrations in global climate 65 ma to present. *Science*, **292**(5517), 686–693.

van der Zwan, C., 2002. The impact of milankovitch-scale climatic forcing on sediment supply. *Sed. Geol.*, **147**, 271–294.

Received 18 November 2014; revised version accepted 1 September 2015

